Acta Biochimica Polonica

Vol. 44 No. 3/1997

519–526

QUARTERLY

The determination of thymopoietin conformation based on X-ray structure of a discontinuous thymopoietin-like motif of G-actin

Ignacy Z. Siemion✉, Iwona Strug and Zbigniew Szewczuk

Department of Chemistry, University of Wrocław, F. Joliot-Curie 14, 50-383 Wrocław, Poland

Keywords: G-actin, thymopoietin, thymopoietin-like motif

The biologically active conformation of thymopoietin, based on X-ray data reported for discontinuous thymopoietin-like motif of G-actin, is proposed. The conformation is compared with that resulting from the prediction made by the method of Chou & Fasman (*Annu. Rev. Biochem.* 47, 251–276, 1978) and Rost & Sander (*Methods Enzymol.* 266, 525–539, 1996).

Thymopoietins I and II are two closely related polypeptides, first isolated from bovine thymi [1]. The biological activity of thymopoietins consists in propagation of thymocyte differentiation, which leads to the emergence of different subclasses of T cells after contact with an antigen [2]. During our search for thymopentin-like sequences (thymopentin is the smallest fragment of thymopoietin that exhibits the thymopoietin biological activity [3]), which are present in many regulatory and defence proteins [4–6], we found that there appears a discontinuous thymopoietin-like motif in the molecule of the rabbit muscle contractile protein, G-actin. It is composed of two longer fragments (96–110 and 276–306) and Arg177 and Asn162 residues, corresponding to the fragment Lys-Ser of thymopoietin which connects N-terminal and C-terminal parts of the peptide. Actin is a very conservative protein: the thymopoietin-like motif is preserved in actins from all the investigated species.

The homology between human thymopoietin and rabbit G-actin thymopoietin-like motif is documented in Fig. 1. It is known that thymopoietin affects neuromuscular transmission, evoking abnormalities similar to those observed in the human disease, myasthenia gravis. In the opinion of Goldstein & Schlesinger [7] myasthenia gravis is a consequence of systematic release of thymopoietin from thymus with ensuing neuromuscular block. We assume that these phenomena may be related to the homology between thymopoietin and thymopoietin-like motif of G-actin. It seems probable that both: tymopoietin and actin G interact with the same protein receptor. Thymopoietin could, e.g., influence the polymerisation of G-actin. The last supposition is supported by the fact that the residues 110–112, 285 and 286–289 of G-actin belonging to the thymopoietin-like motif of G-actin, participate in different interactions, which stabilise actin filaments [8]. In such a case, however, the spatial structure of

✉Author for correspondence: Ignacy Z. Siemion, Department of Chemistry, University of Wrocław, ul. F. Joliot-Curie 14, PL-50-383 Wrocław, Poland; tel.: (+71)+20-42-06; fax: (+71)+22-23-48 or 20-42-15; e-mail: SIEMION@CHEM.UNI.WROC.PL

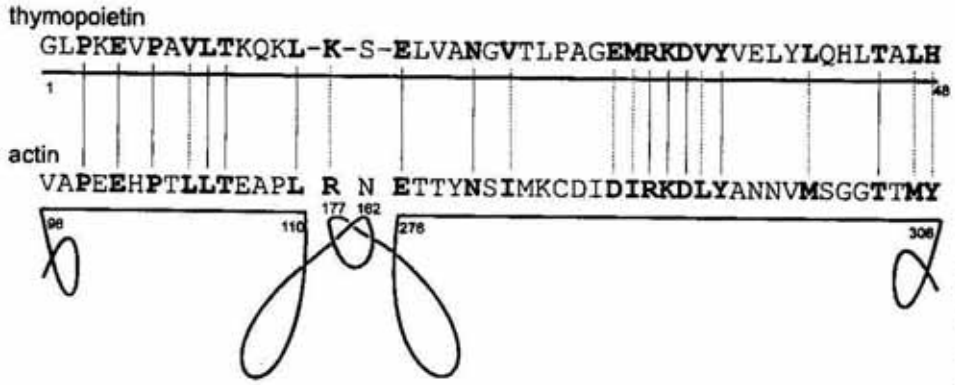

Figure 1. Comparison of the sequence of the human thymopoietin and the thymopoietin-like motif of mammalian G-actin.

- - -, similar residues;
—, the same residues.

thymopoietin-like motif of G-actin should reflect the conformation of thymopoietin, at least its conformation required for the eluciting of the myasthenia gravis phenomenon. Thus, the X-ray structure of thymopoietin-like motif of G-actin can be used as a model for the search of thymopoietin conformation. Such a possibility is examined in this paper by using the molecular modelling methods.

EXPERIMENTAL

Molecular modelling studies

Conformational energy minimisation and dynamics simulation were performed using a HyperChem v. 4.0 software (Autodesc, Inc.) with an Amber Force field. The X-ray structure of rabbit skeletal muscle actin [9] was used as the starting structure in the modelling. The minimum energy conformation of thymopoietin was computed by two independent methods:

Method A. The 1–15 and 18–48 fragments of human thymopoietin were endowed with conformational angles ϕ and ψ resulting from the X-ray structure of the respective fragments (96–110 and 276–306) of rabbit G-actin. The Leu-Lys-Ser-Glu tetrapeptide moiety was in the conformation enabling the connection of two fragments. The potential energy of the system was minimised *in vacuo*, i.e. without respect to the external interactions of the peptide.

Method B. Within the G-actin molecule a cavity was formed by removing the residues belonging to the thymopoietin-like motif (the fragments 96–110 and 276–306 and residues Arg177 and Asn162). The Met176 residue was also removed to avoid sterical constraints. The continuous thymopoietin sequence was located in this cavity and its ends were assumed to be covalently bound to the residues 95 and 307 of G-actin, respectively. The particular amino-acid residues of thymopoietin sequence were endowed with conformational characteristics of the respective residues of G-actin; the conformation of the binding element Leu15-Lys-Ser-Glu18 was adjusted to such a fragment of G-actin which enabled creation of a continuous thymopoietin segment within the G-actin cavity. The conformational energy of the thymopoietin segment was minimised considering all variables, taking the conformation of all other amino-acid residues invariable, i.e. assuming that the G-actin residues form a rigid matrix for the thymopoietin segment.

Molecular dynamics simulation

A 100000-step (100 ps) dynamic simulation was carried out for the thymopoietin segment inserted into the G-actin matrix in the minimum energy conformation. The simulation was performed at the constant temperature of 300 K, followed by cooling the system to 0 K over the time period of 10 ps. The same procedure was used for isolated thymopoietin endowed with a conformation resulting from method B.

The prediction of thymopoietin conformation from its sequence

The prediction of thymopoietin secondary structure from its sequence was carried out

by the PHD (**Profile** network prediction **HeiD**elberg) system of Rost & Sander [10–12].

RESULTS

The mutual spatial orientation of G-actin fragments which constitute the thymopoietin-like motif of the protein, is shown in Fig. 2. It can be seen from this figure that limited changes of the conformational angles ϕ and ψ of Leu110, Asn162, Arg177 and Glu276 enable formation of the continuous thymopoietin-like segment within the molecule of G-actin. The conformational angles of the residues of G-actin used in the computation of the thymopoietin conformation, are summarised in Table 1. In the same Table the values of ϕ and ψ angles calculated for thymopoietin by methods A and B are given. As we can see from these data, both methods lead to very similar structures, although the conformation calculated by method A is closer to that existing in G-actin than the conformation computed by method B.

The most characteristic pattern of the computed thymopoietin conformation is the presence of two helical fragments (Val20–Leu26 fragment on one side, and Gly29–Val37 fragment on the other side), connected by the irregular loop created by the Pro-Ala moiety. The first of these fragments exists in α-helical conformation while the second is more extended and resembles rather 3_{10} helix. The N-terminal part of the molecule is less regular. Its structurally organised elements consist of the Leu4–Glu5 helix, inverse γ-turns on Pro7 and Lys14, a γ-turn on Leu15, and a distorted β structure element of the dipeptide moiety Ala8-Val9. The conformation of thymopoietin (computed by method B) is depicted in Fig. 3.

This conformation, corresponding to the local minimum energy found by the method discussed above, was used as a starting one for the molecular dynamics simulation. The obtained structure is shown in Fig. 4. As we can see from this picture, the thymopoietin sequence inserted into a G-actin molecule shows a distinct conformational stability. The minor changes of conformation are easy to observe for N-terminal and central parts of the thymopoietin segment. In particular, the stability of the helix present in the Arg32-Glu38 fragment is worth noting. Of course, the conformational stability of the thymopoietin segment may be in this case due to the influence of the G-actin rigid matrix: the insertion of thymopoietin into the G-actin

Table 1. Torsional angles of a discontinuous thymopoietin-like motif in G-actin molecule taken from the X-ray structure of rabbit skeletal muscle actin ([9], panel A) and our models of biologically active conformations of thymopoietin obtained after energy minimalization *in vacuo* (panel B) and within the actin molecule (panel C)

A			B			C	
aa	ϕ	ψ	aa	ϕ	ψ	ϕ	ψ
Val 96		161	Gly 1		149		139
Ala 97	-92	127	Leu 2	-74	132	-65	145
Pro 98	-67	-29	Pro 3	-71	-42	-55	-20
Glu 99	-67	2	Lys 4	-38	-45	-51	-65
Glu 100	-127	21	Glu 5	-74	-32	-70	-28
His 101	-125	127	Val 6	-103	119	-125	85
Pro 102	-69	143	Pro 7	-55	104	-67	68
Thr 103	-122	115	Ala 8	-82	88	-153	161
Leu 104	-96	123	Val 9	-60	139	-66	122
Leu 105	-109	165	Leu 10	-134	151	-86	-176
Thr 106	-122	152	Thr 11	-97	176	-57	150
Glu 107	-127	172	Lys 12	-154	156	-160	-174
Ala 108	-85	162	Gln 13	-68	136	-140	154
Pro 109	-38	-58	Lys 14	-69	68	-80	67
Leu 110	-119		Leu 15	27	-93	55	-107
Arg 177			Lys 16	-159	-160	-145	137
Asn 162			Ser 17	176	78	160	63
Glu 276		-35	Glu 18	-115	-156	-97	146
Thr 277	-71	-38	Leu 19	64	82	80	130
Thr 278	-52	-46	Val 20	-37	-55	-51	-54
Tyr 279	-68	-49	Ala 21	-49	-57	-51	-53
Asn 280	-64	-32	Asn 22	-62	-45	-58	-54
Ser 281	-59	-45	Gly 23	-41	-48	-52	-49
Ile 282	-69	-46	Val 24	-83	-30	-62	-51
Met 283	-77	11	Thr 25	-73	-35	-169	-82
Lys 284	-100	-6	Leu 26	-57	-54	-57	-48
Cys 285	-96	169	Pro 27	-70	-175	-80	-170
Asp 286	-62	145	Ala 28	-52	135	-66	-179
Ile 287	-58	-44	Gly 29	-48	-43	-63	-60
Asp 288	-69	-27	Glu 30	-57	-25	-52	-53
Ile 289	-90	-11	Met 31	-87	-2	-49	-29
Arg 290	-63	-27	Arg 32	-67	-59	-51	-38
Lys 291	-68	29	Lys 33	-47	-45	-65	-49
Asp 292	-69	-54	Asp 34	-61	-54	-72	-35
Leu 293	-53	-40	Val 35	-70	-35	-57	-50
Tyr 294	-66	-32	Tyr 36	-57	-44	-59	-42
Ala 295	-90	11	Val 37	-66	-61	-64	-70
Asn 296	-148	65	Glu 38	-79	56	-77	68
Asn 297	-92	100	Leu 39	-74	71	-71	71
Val 298	-98	135	Tyr 40	-70	69	-56	115
Met 299	-105	136	Leu 41	-69	131	-165	162
Ser 300	-145	158	Gln 42	-154	170	-144	165
Gly 301	114	147	His 43	107	136	171	52
Gly 302	-52	-42	Leu 44	-36	-55	-13	-65
Thr 303	-75	-8	Thr 45	-43	-46	-41	-42
Thr 304	-92	10	Ala 46	-64	-16	-94	-65
Met 305	-87	-16	Leu 47	-50	-41	-79	72
Tyr 306	-47		His 48	-78		49	

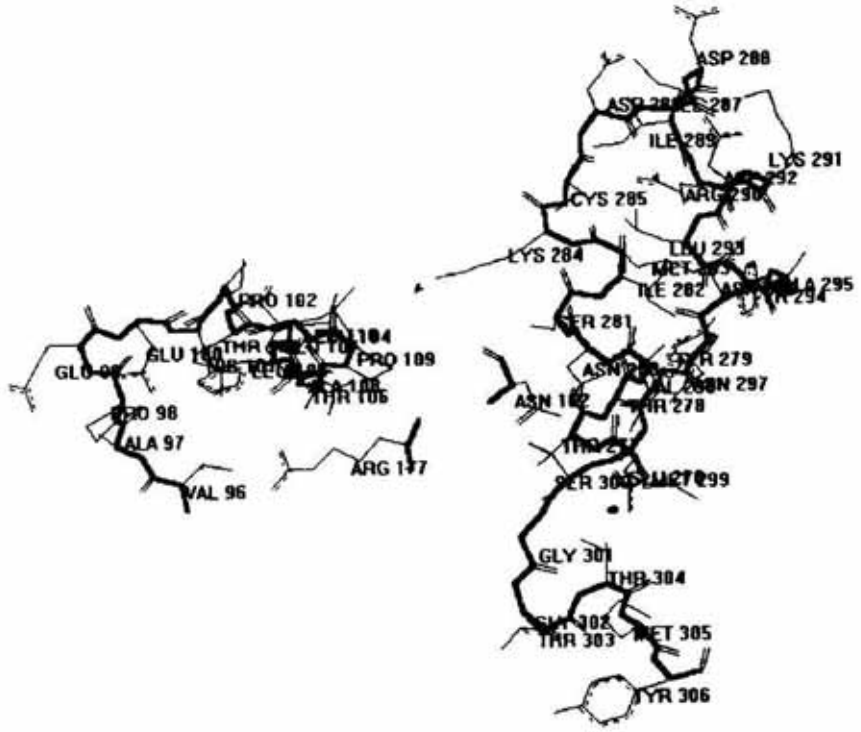

Figure 2. Mutual spatial orientation of the G-actin fragments constituting the thymopoietin-like motif.

The thick lines correspond to the elements of peptide backbone.

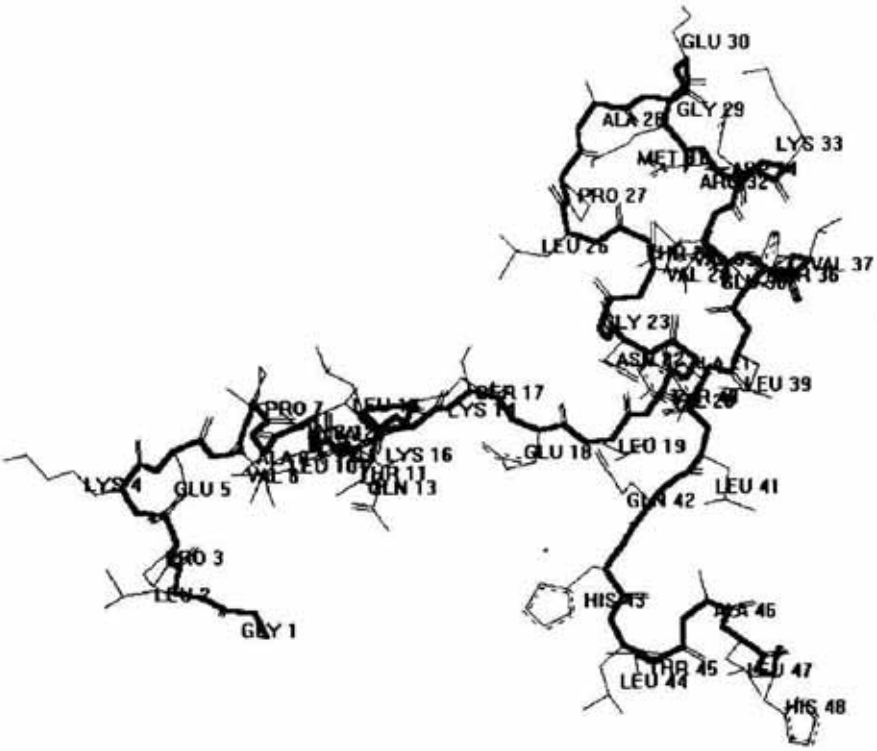

Figure 3. Conformation of the thymopoietin resulting from its insertion into the G-actin molecule and potential energy minimisation.

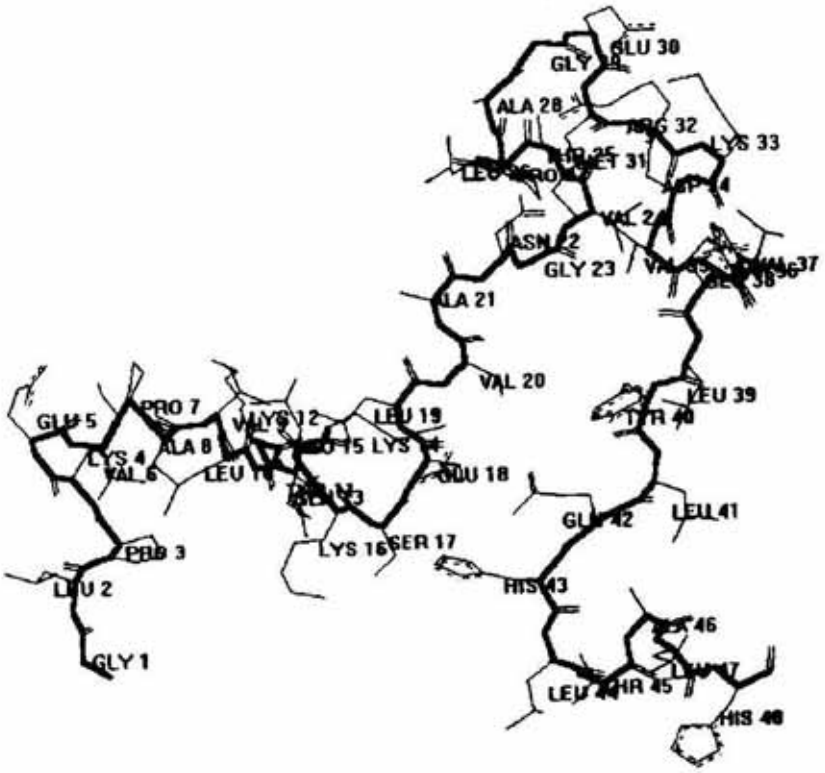

Figure 4. Conformation of the thymopoietin inserted into the G-actin molecule after molecular dynamics simulation procedure.

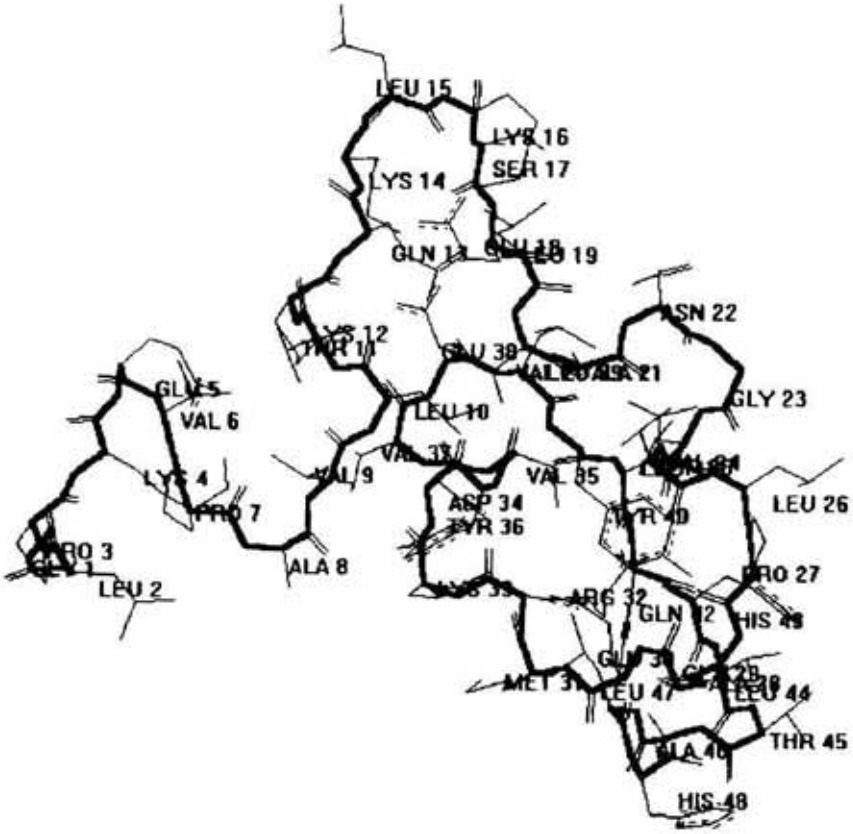

Figure 5. Conformation of the isolated thymopoietin peptide chain after molecular dynamics simulation procedure.

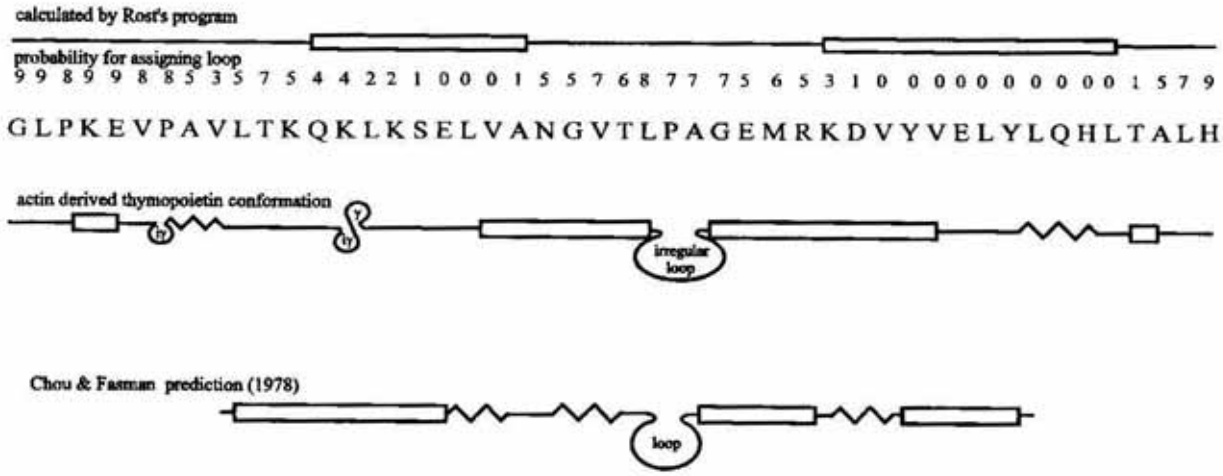

Figure 6. Comparison of conformations of the thymopoietin molecule predicted by Chou & Fasman program, calculated by Rost & Sander program and derived from the X-ray data of actin molecule.

The boxes on the Figure represent the helical fragments, the zigzag lines — β-structure fragments; iγ illustrates inverse γ-turn and γ shows a γ-turn.

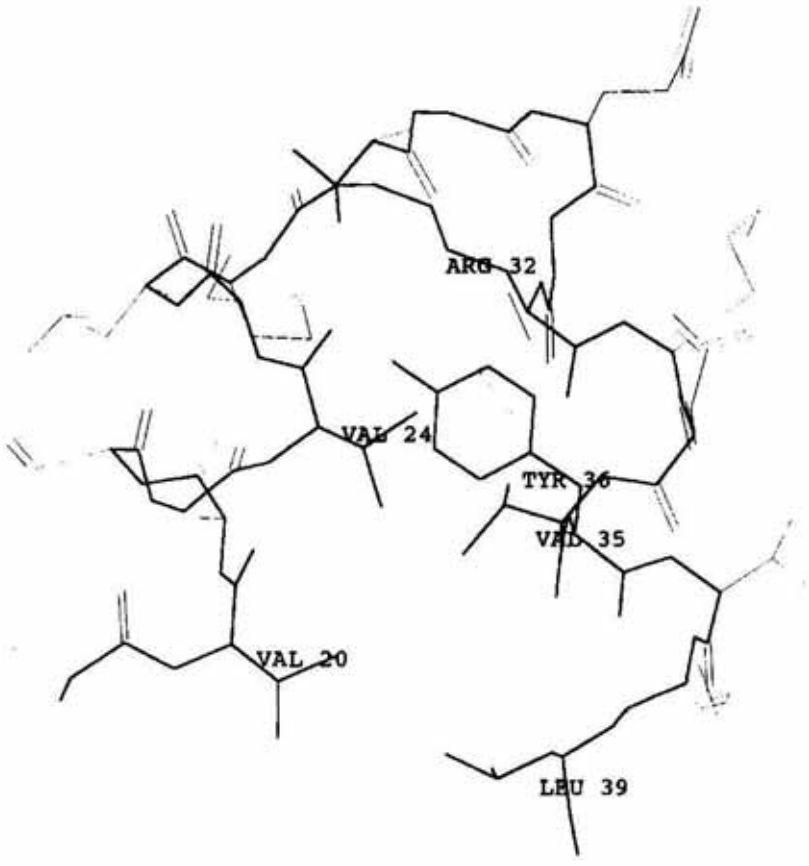

Figure 7. Hydrophobic core made by the side chains of hydrophobic amino acids of two helices predicted by our model of the thymopoietin conformation.

molecule could strongly reduce its conformational freedom. This assumption is supported by the molecular dynamics studies performed for isolated thymopoietin, endowed with the conformation shown in Fig. 3. In this case the result of simulation is a complete collapse of the initial structure (see Fig. 5).

DISCUSSION

We compared the computed thymopoietin conformation with that predicted from its amino-acid sequence. Such a prediction was done in 1978 by Chou & Fasman [13]. It presented, however, only a limited similarity

to our proposal (see Fig. 6). However, the localisation of a loop, accompanied by adjacent helical fragments, is exactly the same in both these propositions. The method of prediction published by Rost & Sander [10–12] gives a result more acceptable from our point of view. The prediction anticipates the presence of two prolonged helical fragments in the thymopoietin molecule, separated by a sequence for which a high probability for loop appearance was predicted. The helical fragments resulting from the prediction coincide in part with the helical fragments postulated by us; also our localisation of the loop corresponds very well with the predicted one. Thus, there is quite a good correspondence between our model of the thymopoietin conformation and its predicted structure.

A very interesting feature of the pattern of the conformation proposed by us is that the hydrophobic side chains of Val20 and Val24 of the first helical fragment and Val35 and Tyr36 of the second helix, as well as Leu39 side chain, are oriented into the internal space between the interacting helices, forming a kind of hydrophobic core. This situation is reflected in Fig. 7. The postulated spatial proximity of the mentioned residues would enable the examination of our model of thymopoietin conformation by NMR methods. Such a work is now in progress in our laboratory.

REFERENCES

1. Goldstein, G. (1974) Isolation of bovine thymin: A polypeptide hormone of thymus. *Nature* **247**, 11–14.
2. Barch, R.S. & Goldstein, G. (1974) Induction of T cell differentiation *in vitro* by thymin, a purified polypeptide hormon of the thymus. *Proc. Natl. Acad. Sci. U.S.A.* **71**, 1474–1478.
3. Goldstein, G., Audhya, T. & Heavner, G.A. (1981) Thymopoietins: Structural studies of these immunoregulatory polypeptides; in *Peptides, Synthesis-Structure-Function, Proc. 7th Amer. Pept. Symp., Pierce, Rockford,* pp. 535–539.
4. Siemion, I.Z., Słoń, J. & Wieczorek, Z. (1995) The immunosuppressive mini-domain of human lactoferrin. *J. Peptide Sci.* **1**, 295–302.
5. Szewczuk, Z., Siemion, I.Z. & Wieczorek, Z. (1996) Immunological properties of the thymopentin-like fragments of HLA-DQ. *Molec. Immunol.* **33**, 903–908.
6. Wieczorek, Z., Słoń, J., Kluczyk, A., Zbozień, R., Stefanowicz, P. & Siemion, I.Z. (1995) The immunomodulatory diversity of the proteins of transforming growth factor β (TGF β) family. *Int. J. Peptide Protein Res.* **46**. 113–118.
7. Goldstein, G. & Schlesinger, D.H. (1975) Thymopoietin and myasthenia gravis: Neostigmine-responsive neuromuscular block produed in mice by a synthetic peptide fragment of thymopoietin. *Lancet* 256–259.
8. Kabsch, W. & Vandekerckove, J. (1992) Structure and function of actin. *Annu. Rev. Biophys. Biomol. Struct.* **21**, 49–76.
9. Kabsh, W., Mannherz, H.G., Suck, D., Pai, E.F. & Holmes, K.C. (1990) Atomic structure of the actin:DNase I complex. *Nature* **347**, 37–44.
10. Rost, B. & Sander, C. (1993) Prediction of protein secondary structure at better than 70% accuracy. *J. Mol. Biol.* **232**, 584–599.
11. Rost, B. & Sander, C. (1994) Conservation and prediction of solvent accessibility in protein families. *Proteins* **20**, 216–226.
12. Rost, B. & Sander, C. (1996) Predicting one-dimentional protein structure by profile based neural networks. *Methods. Enzymol.* **266**, 525–539.
13. Chou, P.Y & Fasman, G.D. (1978) Empirical predictions of protein conformation. *Annu. Rev. Biochem.* **47**, 251–276.